

AD-A031 234

CALSPAN CORP BUFFALO N Y  
NONLINEAR SMALL-DISTURBANCE EQUATIONS FOR THREE-DIMENSIONAL TRA--ETC(U)  
AUG 76 W J RAE F44620-74-C-0059

F/G 20/4

UNCLASSIFIED

CALSPAN-AB-5487-A-1

AFOSR-TR-76-1082

NL

1 OF 1  
ADA031234



END  
DATE  
FILMED  
11 - 76

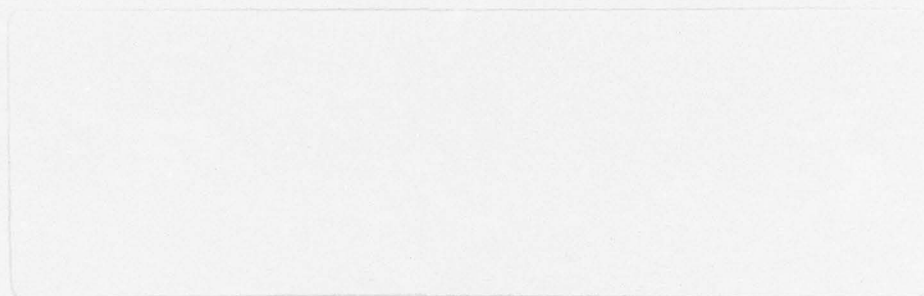
AD A 031 234

AFOSR - TR - 76 - 1082

11

**Calspan**

# Technical Report



DDC  
RECEIVED  
OCT 27 1976  
D

Approved for public release;  
distribution unlimited.

Calspan Corporation  
Buffalo, New York 14221



AIR FORCE OFFICE OF SCIENTIFIC RESEARCH (AFSC)  
NOTICE OF TRANSMITTAL TO DDC  
This technical report has been reviewed and is  
approved for public release IAW AFR 190-12 (7b).  
Distribution is unlimited.  
A. D. BLOSE  
Technical Information Officer

|                                 |               |                                     |
|---------------------------------|---------------|-------------------------------------|
| DDC                             | White Section | <input checked="" type="checkbox"/> |
| UNANNOUNCED                     | But: Section  | <input type="checkbox"/>            |
| IDENTIFICATION                  |               |                                     |
| BY                              |               |                                     |
| DISTRIBUTION/AVAILABILITY CODES |               |                                     |
| Dist.                           | Avail. and/or | SPECIAL                             |
| A                               |               |                                     |

# Calspan

*NONLINEAR SMALL-DISTURBANCE EQUATIONS FOR  
THREE-DIMENSIONAL TRANSONIC FLOW THROUGH A  
COMPRESSOR BLADE ROW*

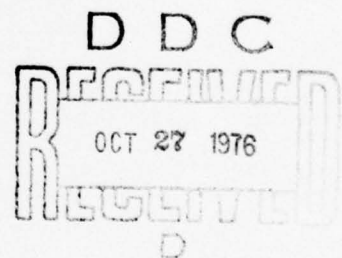
William J. Rae  
Calspan Report No. AB-5487-A-1

AUGUST 1976

Prepared For:

AIR FORCE OFFICE OF SCIENTIFIC RESEARCH  
BOLLING AIR FORCE BASE, D.C. 20332

CONTRACT NO. F44620-74-C-0059  
INTERIM SCIENTIFIC REPORT



CONDITIONS OF REPRODUCTION

Reproduction, translation, publication, use and disposal in whole or in part by or for the United States Government is permitted.

Approved for public release; distribution unlimited.

Calspan Corporation  
Buffalo, New York 14221

Qualified requestors may obtain additional copies from the Defense Documentation Center, all others should apply to the National Technical Information Service.

UNCLASSIFIED

SECURITY CLASSIFICATION OF THIS PAGE (When Data Entered)

9 Technical rept.

REPORT DOCUMENTATION PAGE

READ INSTRUCTIONS BEFORE COMPLETING FORM

|  |  |  |
|--|--|--|
| 1. REPORT NUMBER<br>18 AFOSR - TR - 76 - 1082 -  | 2. GOVT ACCESSION NO.  | 3. RECIPIENT'S CATALOG NUMBER                    |
| 4. TITLE (and Subtitle)<br>6 NONLINEAR SMALL-DISTURBANCE EQUATIONS FOR THREE-DIMENSIONAL TRANSONIC FLOW THROUGH A COMPRESSOR BLADE ROW     | 5. TYPE OF REPORT & PERIOD COVERED<br>INTERIM  |  |
| 7. AUTHOR(s)<br>10 WILLIAM J. RAE  | 14 CALSPAN<br>15 F44620-74-C-0059 NEW  | 6. PERFORMING ORG. REPORT NUMBER<br>-AB-5487-A-1 |
| 9. PERFORMING ORGANIZATION NAME AND ADDRESS<br>CALSPAN CORPORATION<br>P O BOX 235<br>BUFFALO, NEW YORK 14221 ✓                             | 10. PROGRAM ELEMENT, PROJECT, TASK AREA & WORK UNIT NUMBERS<br>16 AF-9781-01 17 978101<br>61102F | 8. CONTRACT OR GRANT NUMBER(s)                   |
| 11. CONTROLLING OFFICE NAME AND ADDRESS<br>AIR FORCE OFFICE OF SCIENTIFIC RESEARCH/NA<br>BUILDING 410<br>BOLLING AIR FORCE BASE, D C 20332 | 12. REPORT DATE<br>14 Aug 76   | 13. NUMBER OF PAGES<br>39 12 43 p.               |
| 14. MONITORING AGENCY NAME & ADDRESS (if different from Controlling Office)  | 15. SECURITY CLASS. (of this report)<br>UNCLASSIFIED   | 15a. DECLASSIFICATION/DOWNGRADING SCHEDULE       |

16. DISTRIBUTION STATEMENT (of this Report)  
Approved for public release; distribution unlimited.

17. DISTRIBUTION STATEMENT (of the abstract entered in Block 20, if different from Report)

18. SUPPLEMENTARY NOTES

19. KEY WORDS (Continue on reverse side if necessary and identify by block number)  
TURBOMACHINERY  
COMPRESSORS  
TRANSONIC FLOW  
EQUATIONS

20. ABSTRACT (Continue on reverse side if necessary and identify by block number)  
A derivation is given of the nonlinear, small-disturbance equations governing three-dimensional transonic flow through a fan or compressor rotor. These equations represent the counterpart, for turbomachinery flows, of the small-disturbance equations appropriate to an isolated airfoil. Thus, they facilitate the application to turbomachinery flows of the many numerical solution methods developed in recent years for isolated-airfoil problems. Boundary conditions for design and off-design conditions are formulated, at a level of approximation consistent with the small-disturbance field equations. An order-of-magnitude

bpg

**UNCLASSIFIED**

SECURITY CLASSIFICATION OF THIS PAGE(When Data Entered)

analysis is presented, which reveals the transonic similarity parameters for flow in blade rows of low and high solidity. The validity of a rectilinear transonic shear flow as a representation of the flow through a fan or rotor is also discussed.

**UNCLASSIFIED**

SECURITY CLASSIFICATION OF THIS PAGE(When Data Entered)

## ABSTRACT

A derivation is given of the nonlinear, small-disturbance equations governing three-dimensional transonic flow through a fan or compressor rotor. These equations represent the counterpart, for turbomachinery flows, of the small-disturbance equations appropriate to an isolated airfoil. Thus they facilitate the application to turbomachinery flows of the many numerical solution methods developed in recent years for isolated-airfoil problems.

Boundary conditions for design and off-design conditions are formulated, at a level of approximation consistent with the small-disturbance field equations. An order-of-magnitude analysis is presented, which reveals the transonic similarity parameters for flow in blade rows of low and high solidity.

The validity of a rectilinear transonic shear flow as a representation of the flow through a fan or rotor is also discussed.

## LIST OF SYMBOLS

|                             |  |
|-----------------------------|--|
| $a^2$                       | square of the local sound speed  |
| $B$                         | number of blades   |
| $C_a$                       | axial projection of the blade chord  |
| $\hat{e}$                   | unit vector  |
| $h$                         | static enthalpy  |
| $H$                         | total enthalpy   |
| $I$                         | modified enthalpy function, see Equation (12)  |
| $L_T$                       | $2\pi G / B$   |
| $M_{\infty}$                | Mach number, $U_{\infty} / a_{\infty}$   |
| $n$                         | distance normal to an undisturbed streamline, at constant $r$                                |
| $\eta(s)$                   | blade shape, see Equation (43)   |
| $p$                         | static pressure  |
| $R, r$                      | radial coordinate  |
| $s$                         | entropy, Equation (13). Elsewhere, distance along an undisturbed streamline, at constant $r$ |
| $t$                         | time   |
| $U_{\infty}$                | axial component of approach flow   |
| $u, v, w$                   | perturbation velocity components, see Equation (18)  |
| $\bar{u}, \bar{v}, \bar{w}$ | normalized perturbation velocity components, $u/a_{\infty}, v/a_{\infty}, w/a_{\infty}$      |
| $u_s, u_n$                  | perturbation velocity components along and normal to the undisturbed streamline directions   |
| $V$                         | fluid velocity in absolute coordinates   |
| $\mathcal{V}$               | fluid velocity in space-fixed coordinates  |
| $W$                         | fluid velocity in blade-fixed coordinates  |
| $Z$                         | $\omega^x / U_{\infty}$  |
| $( )_h$                     | denotes evaluation at the hub  |
| $( )_t$                     | denotes evaluation at the tip  |
| $( )_{u,l}$                 | denotes evaluation on the upper, lower surface of the blade                                  |
| $( )_{\infty}$              | denotes evaluation far upstream  |
| $( )_1$                     | denotes space-fixed coordinates  |
| $( )_2$                     | denotes absolute coordinates   |
| $\gamma$                    | specific heat ratio  |
| $\xi$                       | $\theta - z$ , see Equation (38)   |

LIST OF SYMBOLS (Cont'd)

- $\rho$  dimensionless radius,  $\omega r / U_\infty$
- $\rho$  mass density
- $\phi$  dimensional perturbation potential
- $\phi$  dimensional perturbation potential, in the space-fixed coordinates
- $\bar{\phi}$  dimensionless perturbation potential,  $\omega \phi / U_\infty^2$
- $\psi(r)$  angle between axis of symmetry and undisturbed streamline direction, at constant radius
- $\vec{\omega}_B$  angular velocity of the rotor in absolute coordinates
- $\omega$  angular velocity of the flow, as seen by a blade-fixed observer.

## TABLE OF CONTENTS

| <u>Section</u> |   | <u>Page No.</u> |
|----------------|---|-----------------|
|                | INTRODUCTION .....                              | 1               |
| I              | THE BASIC EQUATIONS .....                       | 3               |
|                | Coordinate Systems .....                        | 3               |
|                | Equations of Motion .....                       | 3               |
| II             | SMALL-DISTURBANCE EQUATIONS .....               | 8               |
|                | Transonic Shear-Flow Approximation .....        | 13              |
|                | Velocity-Component Equations .....              | 14              |
|                | Potential Equation .....                        | 15              |
|                | Coordinate Transformation .....                 | 16              |
|                | Boundary Conditions at the Blade Surfaces ..... | 18              |
|                | Periodicity and Farfield Conditions .....       | 20              |
|                | Farfield Conditions .....                       | 23              |
| III            | SIMILARITY PARAMETERS .....                     | 25              |
|                | CONCLUDING REMARKS .....                        | 29              |

## INTRODUCTION

Axial-flow compressors have been operated for many years in the transonic range, i.e., such that the resultant of the axial approach velocity of the flow and the circumferential velocity of the blades is sonic somewhere between the hub and the tip. Under these circumstances, an observer riding on one of the blades sees a mixed flow, in which a subsonic region near the hub exists side-by-side with a supersonic region near the tip. These two regions interact, making three-dimensionality an essential feature of the flow. The addition of this feature to the complexities already inherent in the transonic character of the flow makes the problem a very formidable one.

Despite these complications, transonic compressors have given satisfactory performance, and in recent years the conflicting demands of increased compression per stage, with decreased weight and noise generation, have continued to place great emphasis on the flow field problems of these devices, which are inherently three-dimensional and nonlinear.<sup>1</sup>

With one or two exceptions, most of the existing studies of these flow fields have separated the three-dimensionality and the nonlinearity. Thus, there are extensive studies in which the nonlinearity is accounted for, but in a two-dimensional approximation (see, for example, References 2 and 3) and a lesser number in which the three-dimensionality is studied, but in a linear approximation (References 4 and 5 are typical). The nonlinear, two-dimensional solutions are often applied in an iterative manner, starting with an axisymmetric calculation, to determine a stream surface location in a meridional plane. Then the flow in the blade-to-blade plane is calculated. The success of the latter calculation is seriously affected by the presence of shock waves in the field; the problem of locating them, and of adjusting their locations on subsequent iterations has been found to be very difficult. Thus, the three-dimensionality and the nonlinearity become especially hard to handle, even in an iterative way, when transonic flow conditions occur.

In contrast, many calculations of the transonic flow over isolated airfoils have appeared in recent years.<sup>7-14</sup> These methods have reached a stage of development that allows three-dimensionality and nonlinearity to be included simultaneously. However, it appears that most of these significant advances have not yet been successfully carried over to the calculation of turbomachinery flows.

The purpose of the present study is to adapt the isolated-airfoil computational techniques to the problems of turbomachinery flows. As the first step in this process, the appropriate nonlinear small-disturbance equations are derived in this paper. These equations are presented in a form that facilitates application of virtually all of the isolated-airfoil numerical techniques. The successful adaptation of these techniques to the conditions of flow in a rotating blade row is a logical first step in the exploitation of the whole range of methods for solving the fully nonlinear problem.

The first section below retraces the derivation of the basic equations, paying careful attention to the conditions under which the flow seen by a blade-fixed observer may be considered steady. The results of this section shed light on the approximation implicit in the use of a rectilinear transonic shear flow as a model of the flow in a transonic compressor blade row.

The second section takes up the special case in which the flow in blade-fixed coordinates consists of small disturbances from a helical stream. The leading nonlinear terms which govern the transonic character of the flow are retained, in a fully three-dimensional treatment.

Since the problem contains several small parameters (including the departure of the local Mach number from unity and also the geometric and loading parameters that produce the small disturbances from helical flow) an order-of-magnitude analysis is needed, to identify the relative sizes of the parameters that may consistently be retained. This analysis is presented in Section III. The concluding section reviews some of the implications which the present results will have for later numerical work, and extensions to more fully nonlinear approximations.

## I. THE BASIC EQUATIONS

The purpose of the present work is to facilitate the application, to turbomachinery flowfields, of a number of numerical methods which were developed originally for external flows over isolated bodies. Thus, although the equations of motion for turbomachinery flows are well known, nevertheless there is a need to retrace their derivation, in order to display the forms analogous to those that have been used in numerical studies of external flows.

### Coordinate Systems

Several coordinate systems can be used to describe the flow in a compressor blade row. The first, called "space-fixed", is one in which the rotor advances and rotates. The flow in this coordinate system is always time-dependent. The subscript ( )<sub>1</sub> is used in this paper to designate these coordinates. (See Figure 1.)

The second system can be thought of as being fixed in the engine mount. In these coordinates, the blade row rotates, but does not advance. Following Wu<sup>15</sup>, these coordinates are referred to as "absolute". They are designated here by the subscript ( )<sub>2</sub>. The flow is unsteady in these coordinates. (See Figure 2.)

A third system of coordinates, introduced below, has an origin fixed on one of the blades. This system, referred to by Wu as "relative", is denoted in this paper by the term "blade-fixed", and by coordinate symbols with no subscript. Under certain conditions, the flow in these coordinates may be regarded as steady.

### Equations of Motion

In the absolute coordinates, the component forms of the continuity and momentum equations are:

$$\frac{\partial \rho}{\partial t_2} + \frac{\partial}{\partial x_2} (\rho V_x) + \frac{1}{r_2} \frac{\partial}{\partial r_2} (r_2 \rho V_r) + \frac{1}{r_2} \frac{\partial}{\partial \theta_2} (\rho V_\theta) = 0 \quad (1)$$

$$\frac{\partial V_x}{\partial t_2} + V_x \frac{\partial V_x}{\partial x_2} + V_r \frac{\partial V_x}{\partial r_2} + \frac{V_\theta}{r_2} \frac{\partial V_x}{\partial \theta_2} + \frac{1}{\rho} \frac{\partial p}{\partial x_2} = 0 \quad (2)$$

$$\frac{\partial V_r}{\partial t_2} + V_x \frac{\partial V_r}{\partial x_2} + V_r \frac{\partial V_r}{\partial r_2} - \frac{V_\theta^2}{r_2} + \frac{V_\theta}{r_2} \frac{\partial V_r}{\partial \theta_2} + \frac{1}{\rho} \frac{\partial p}{\partial r_2} = 0 \quad (3)$$

$$\frac{\partial V_\theta}{\partial t_2} + V_x \frac{\partial V_\theta}{\partial x_2} + V_r \frac{\partial V_\theta}{\partial r_2} + \frac{V_\theta}{r_2} \frac{\partial V_\theta}{\partial \theta_2} + \frac{V_\theta V_r}{r_2} + \frac{1}{r_2 \rho} \frac{\partial p}{\partial \theta_2} = 0 \quad (4)$$

The quantities  $x_2$ ,  $r_2$ ,  $\theta_2$  are cylindrical coordinates, with  $x_2$  along the axis of the blade row,  $r_2$  in the radial direction, and  $\theta_2$  measured positive in the right-handed sense (see Figure 1).

Next, these equations are written in blade-fixed coordinates, using velocity components relative to the blades. The relative velocity  $\vec{W}$  is given by:

$$\vec{V} = \vec{W} + \vec{\omega}_B \times \vec{r} \quad (5)$$

where  $\vec{\omega}_B$  is the angular velocity of the blade row:

$$\vec{\omega}_B = \omega_B \hat{e}_x$$

where  $\hat{e}_x$  is a unit vector in the  $x$ -direction. Then

$$\vec{\omega}_B \times \vec{r} = \omega_B r \hat{e}_\theta, \quad \vec{V} = \vec{W} + \omega_B r \hat{e}_\theta \quad (6)$$

$$\vec{W} = \{W_x, W_r, W_{\theta_3}\}; \quad W_x = V_x, \quad W_r = V_r, \quad W_{\theta_3} = V_{\theta_3} - \omega_B r$$

The blade-fixed coordinates (see Figure 3) are given by

$$\begin{aligned} x &= x_2 & \frac{\partial}{\partial x_2} &= \frac{\partial}{\partial x} \\ r &= r_2 & \frac{\partial}{\partial r_2} &= \frac{\partial}{\partial r} \\ \theta_3 &= \theta_2 - \omega_B t_2 & \frac{\partial}{\partial \theta_2} &= \frac{\partial}{\partial \theta_3} \\ t &= t_2 & \frac{\partial}{\partial t_2} &= \frac{\partial}{\partial t} - \omega_B \frac{\partial}{\partial \theta_3} \end{aligned} \quad (7)$$

In terms of these variables, the continuity and momentum equations become:

$$\frac{\partial \rho}{\partial t} + \frac{\partial}{\partial x} (\rho W_x) + \frac{1}{r} \frac{\partial}{\partial r} (r \rho W_r) + \frac{1}{r} \frac{\partial}{\partial \theta_3} (\rho W_{\theta_3}) = 0 \quad (8)$$

$$\frac{\partial W_x}{\partial t} + W_x \frac{\partial W_x}{\partial x} + W_r \frac{\partial W_x}{\partial r} + \frac{W_{\theta_3}}{r} \frac{\partial W_x}{\partial \theta_3} + \frac{1}{\rho} \frac{\partial p}{\partial x} = 0 \quad (9)$$

$$\frac{\partial W_r}{\partial t} + W_x \frac{\partial W_r}{\partial x} + W_r \frac{\partial W_r}{\partial r} + \frac{W_{\theta_3}}{r} \frac{\partial W_r}{\partial \theta_3} - \frac{W_{\theta_3}^2}{r} - 2\omega_B W_{\theta_3} - \omega_B^2 r + \frac{1}{\rho} \frac{\partial p}{\partial r} = 0 \quad (10)$$

$$\frac{\partial W_{\theta_3}}{\partial t} + W_x \frac{\partial W_{\theta_3}}{\partial x} + W_r \frac{\partial W_{\theta_3}}{\partial r} + 2\omega_B W_r + \frac{W_{\theta_3}}{r} \frac{\partial W_{\theta_3}}{\partial \theta_3} + \frac{W_r W_{\theta_3}}{r} + \frac{1}{\rho} \frac{\partial p}{\partial \theta_3} = 0 \quad (11)$$

Note that these equations are unchanged if the signs of all the angular variables are reversed. This is equivalent (see Figure 3) to reversing the sense of the angular variable and the angular velocity component, and to interpreting  $\omega$  as the angular velocity of the flow relative to the blades:

$$\omega_{\theta} = -\omega_{\theta_3} ; \theta = -\theta_3 + \text{const} ; \omega = -\omega_B$$

If there are no flowfield disturbances which vary with  $\theta_2$  in the absolute coordinates, then the flow in the blade-fixed coordinates may be taken as steady. This means that there can be no rows of stators or inlet guide vanes nearby, nor any non-axisymmetric inlet distortion. Thus, strictly speaking, the rotor must be completely isolated. This restriction is very carefully stated by Wu (Reference 15, p. 12) and by Vavra (Reference 16, pp. 111-112).

In actual practice, it may be expected that the steady-flow approximation in blade-fixed coordinates will have acceptable accuracy whenever the neighboring stators are several chord lengths away. The fact that this approximation has been used routinely for many years (see, for example, Reference 17) for design purposes, even at very small rotor-stator spacings, is evidence that the steady-flow approximation is satisfactory for at least some purposes. In the remainder of the present work, this approximation will be adopted, in common with the bulk of existing work on turbomachinery flowfields. Thus, the basic equations used are Eqs. (8)-(11), with time derivatives set equal to zero,  $\theta_3$  replaced by  $\theta$ , and  $-\omega_B$  replaced by  $\omega$ .

The law of conservation of energy, expressed in the absolute coordinates, states that the change in total enthalpy per unit mass  $H = h + \frac{V^2}{2}$  on passing through the blade row is equal to the mechanical work done by the blade row on the fluid. In blade-fixed coordinates, it is much more convenient to use a quantity  $I$ , defined as

$$I = h + \frac{w^2}{2} - \frac{(\omega r)^2}{2} \quad (12)$$

Wu<sup>15</sup> has shown by straightforward manipulations that  $I$  satisfies the equation

$$\frac{DI}{Dt} = T \frac{Ds}{Dt} + \frac{1}{\rho} \frac{\partial p}{\partial t} \quad (13)$$

where  $S$  is the entropy per unit mass, and  $D/Dt$  denotes the convective derivative. Thus, in a flow which is steady, and where the entropy is constant along streamlines, the quantity  $I$  will also be constant along streamlines.

These approximations are adopted here. Thus using

$$h = \frac{a^2}{\gamma-1}, \quad a^2 = \frac{\gamma p}{\rho}$$

The conservation of quantity  $I$  along streamlines becomes:

$$\frac{a_\infty^2}{\gamma-1} + \frac{w_\infty^2}{2} - \frac{(\omega r_\infty)^2}{2} = \frac{a^2}{\gamma-1} + \frac{w^2}{2} - \frac{(\omega r)^2}{2} \quad (14)$$

The terms on the right-hand side of this equation are considered to be evaluated at some arbitrary point  $(x, r, \theta)$  in the flowfield, while those on the left-hand side are evaluated at a related point, on the same streamline, far upstream of the rotor. Since the flow at infinity is assumed not to vary with  $x$  or  $\theta$ , the terms on the left-hand side vary at most with  $r_\infty$ . From Equation (6), it can be seen that

$$\frac{1}{2} w_\infty^2 = \frac{1}{2} \{ u_\infty^2 + 0 + (\omega r_\infty)^2 \}$$

Thus Equation (14) can be written as

$$\frac{a_\infty^2}{\gamma-1} + \frac{u_\infty^2}{2} = \frac{a^2}{\gamma-1} + \frac{w^2}{2} - \frac{(\omega r)^2}{2} \quad (15)$$

In the present work, both  $a_\infty$  and  $u_\infty$  will be taken as constants. It should be stressed, however, that any nonuniformities present in the flow far upstream of the blade row are convected along streamlines. For example, if the gas temperature far upstream had a slight radial variation, then the local sound speed would vary as

$$a^2(r) = a_\infty^2(r_\infty) + \frac{da_\infty^2(r_\infty)}{dr} (r-r_\infty) + \dots$$

where, to first order, the streamline displacement is

$$r-r_\infty = \int_{-\infty}^x \frac{w_r dx}{u_\infty}$$

where the integration is done along an undisturbed streamline.

A single equation, containing only velocity components, can be derived by combining the continuity, momentum, and energy equations. First, using

$$d \ln \rho = d \ln p - d \ln a^2$$

the continuity equation is recast as

$$\frac{\partial w_x}{\partial x} + \frac{1}{r} \frac{\partial}{\partial r} (r w_r) + \frac{1}{r} \frac{\partial w_\theta}{\partial \theta} = - \left\{ w_x \frac{\partial}{\partial x} + w_r \frac{\partial}{\partial r} + \frac{w_\theta}{r} \frac{\partial}{\partial \theta} \right\} \{ \ln p - \ln a^2 \} \quad (16)$$

If the  $x$ ,  $r$ , and  $\theta$  components of the momentum equation are multiplied by  $w_x$ ,  $w_r$ , and  $w_\theta$ , respectively, and added, the resulting equation can be used to eliminate the pressure terms in the equation above, in favor of velocity components. Similarly, the energy equation can be used to replace derivatives of  $a^2$ . The result, after some rearrangement, is:

$$\begin{aligned} a^2 \left\{ \frac{\partial w_x}{\partial x} + \frac{1}{r} \frac{\partial}{\partial r} (r w_r) + \frac{1}{r} \frac{\partial w_\theta}{\partial \theta} \right\} &= w_x \left\{ w_x \frac{\partial w_x}{\partial x} + w_r \frac{\partial w_x}{\partial r} + \frac{w_\theta}{r} \frac{\partial w_x}{\partial \theta} \right\} \\ &+ w_r \left\{ w_x \frac{\partial w_r}{\partial x} + w_r \frac{\partial w_r}{\partial r} + \frac{w_\theta}{r} \frac{\partial w_r}{\partial \theta} - w^2 r \right\} \\ &+ w_\theta \left\{ w_x \frac{\partial w_\theta}{\partial x} + w_r \frac{\partial w_\theta}{\partial r} + \frac{w_\theta}{r} \frac{\partial w_\theta}{\partial \theta} \right\} \quad (17) \end{aligned}$$

## II. SMALL-DISTURBANCE EQUATIONS

Far upstream of the rotor, the components of the velocity vector  $\vec{w}$  approach the axial velocity  $U_\infty \hat{e}_x$  and the wheel velocity  $\omega r \hat{e}_\theta$ , which are the components of the helical approach flow seen by a blade-fixed observer. In what follows, attention is restricted to blade designs which are thin, and essentially aligned with these helical paths, so that only small disturbances from free-stream conditions will occur. These small disturbance quantities are defined as:

$$w_x = U_\infty + u, \quad w_r = v, \quad w_\theta = \omega r + w \quad (18)$$

These expressions are now substituted into Equation (17), and the resulting expression is expanded into terms which are linear, quadratic, and cubic in the small quantities. In addition, the quantity  $a^2$  is written as

$$a^2 = a_\infty^2 + (a^2 - a_\infty^2)$$

where Equation (15) gives

$$a^2 - a_\infty^2 = -(r-1) \left\{ U_\infty u + \omega r w + \frac{u^2 + v^2 + w^2}{2} \right\} \quad (19)$$

After adding and subtracting certain terms, so as to display the vorticity components explicitly, the result is:

$$u_{\infty}^2 \frac{\partial u}{\partial x} + \omega u_{\infty} \frac{\partial u}{\partial \theta} + \omega r u_{\infty} \frac{\partial w}{\partial x} + \omega^2 r \frac{\partial w}{\partial \theta}$$

$$- a_{\infty}^2 \left\{ \frac{\partial u}{\partial x} + \frac{\partial v}{\partial r} + \frac{v}{r} + \frac{1}{r} \frac{\partial w}{\partial \theta} \right\} =$$

$$= -(r-1) \left\{ u_{\infty} u + \omega r w + \frac{u^2 + v^2 + w^2}{2} \right\} \left\{ \frac{\partial u}{\partial x} + \frac{\partial v}{\partial r} + \frac{v}{r} + \frac{1}{r} \frac{\partial w}{\partial \theta} \right\}$$

$$-2 \left\{ u \left( u_{\infty} \frac{\partial u}{\partial x} + \omega \frac{\partial u}{\partial \theta} \right) + v \left( u_{\infty} \frac{\partial v}{\partial x} + \omega \frac{\partial v}{\partial \theta} \right) + w \left( u_{\infty} \frac{\partial w}{\partial x} + \omega \frac{\partial w}{\partial \theta} \right) \right\}$$

$$+ u_{\infty} v \left( \frac{\partial v}{\partial x} - \frac{\partial u}{\partial r} \right) - (u_{\infty} w - \omega r u) \left( \frac{1}{r} \frac{\partial u}{\partial \theta} - \frac{\partial w}{\partial x} \right) - \omega v \left( w + r \frac{\partial w}{\partial r} - \frac{\partial v}{\partial \theta} \right)$$

$$- u \left( u \frac{\partial u}{\partial x} + v \frac{\partial v}{\partial x} + w \frac{\partial w}{\partial x} \right) - v \left( u \frac{\partial u}{\partial r} + v \frac{\partial v}{\partial r} + w \frac{\partial w}{\partial r} \right)$$

$$- \frac{\omega}{r} \left( u \frac{\partial u}{\partial \theta} + v \frac{\partial v}{\partial \theta} + w \frac{\partial w}{\partial \theta} \right)$$

(20)

In deriving this equation, it has been assumed that the entropy is constant along streamlines. Thus the result is not completely general, although it does contain all the possible velocity terms - no small quantities have been neglected yet.

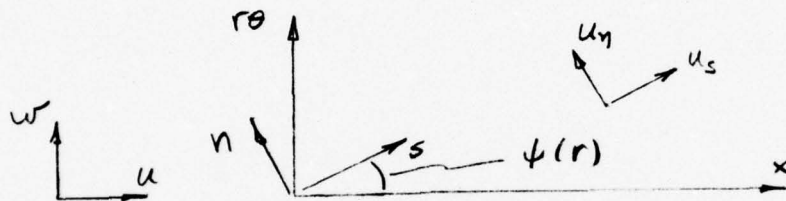
In the remainder of this paper, the disturbance quantities will be assumed small, and the leading terms that must be kept in the transonic range will be sought. The assumptions of small disturbances, and particle - isentropic flow imply that the maximum relative speed of the blades must be only slightly greater than sonic (maximum relative Mach numbers on the order of 1.2 to 1.3, say), so that any shock waves generated will produce negligible changes in entropy. Consistent with this assumption, the flow is taken to be irrotational. Thus, any vorticity produced by shear forces at solid surfaces is assumed to be confined to boundary layers and wakes of negligible thickness. The net effect of these assumptions is to restrict the applicability of the results to thin, lightly loaded blades, operating at tip speeds which are slightly supersonic. In addition, this analysis shares, with the bulk of turbomachinery literature, the steady-flow assumption, which rules out cases where the blade row is located close to any stator rows.

These assumptions impose an upper limit on the range of blade geometries and operating conditions where the present approximation will give good agreement with experiment. Presumably, any design which is to be efficient at transonic speeds must employ thin, lightly loaded blades. In the case of isolated airfoils, there is a large range of thickness, loading, and Mach number where small-disturbance theory compares favorably with experimental data. For the case of turbomachinery flows, the extent of this range remains to be determined, by comparison of its predictions with appropriate experiments.

The approximations inherent in the small-disturbance approximation are further clarified by the work of Kerrebrock<sup>18</sup>, who subdivided the disturbances into pressure, shear, and entropy modes. He states that these three modes are in general coupled to one another in turbomachinery flows, in contrast to their independent, additive behavior in external flows. The present approximation admits only the pressure mode. Shear and entropy disturbances, as noted above, are not present in the inlet flow, and are not created during passage through the blade row.

The absence of entropy disturbances is assured (see Equation 15) by adopting a uniform inlet temperature, while shear disturbances are excluded (see above) by allowing only constant values of  $U_{\infty}$  and  $\omega$ . It is important to note that the radial variation of the resultant velocity does not constitute a shear flow. This point is discussed further below.

The leading terms in Equations (20), which dominate in the transonic range, must now be found. It is clear that the terms on the last three lines can be dropped, as well as the quadratic terms in the first bracket on the third line. In order to determine which of the remaining terms should be kept, it is convenient to use a coordinate system  $s, R, n$  aligned with the helical free-stream:



$$\sin \psi = \frac{+wr/U_{\infty}}{\sqrt{1 + (wr/U_{\infty})^2}}$$

$$\cos \psi = \frac{1}{\sqrt{1 + (wr/U_{\infty})^2}}$$

$$s = x \cos \psi + r\theta \sin \psi = (x + wr^2\theta) / \sqrt{1 + (wr/U_{\infty})^2}$$

$$R = r$$

$$n = -x \sin \psi + r\theta \cos \psi = \frac{r(\theta - \omega x/U_{\infty})}{\sqrt{1 + (wr/U_{\infty})^2}} \quad (21)$$

It should be noted that the  $s, n$  coordinates do not coincide with the local streamline direction, but only with the orientation of the free-stream direction. In general, the local streamlines have a first-order departure from the free-stream direction.

The chain rule expressions for the partial derivatives become:

$$\begin{pmatrix} \frac{\partial}{\partial x} \Big|_{r,\theta} \\ \frac{\partial}{\partial r} \Big|_{x,\theta} \\ \frac{\partial}{\partial \theta} \Big|_{x,r} \end{pmatrix} = \begin{pmatrix} \cos \psi & 0 & -\sin \psi \\ \frac{\partial s}{\partial r} \Big|_{x,\theta} & 1 & \frac{\partial n}{\partial r} \Big|_{x,\theta} \\ r \sin \psi & 0 & r \cos \psi \end{pmatrix} \begin{pmatrix} \frac{\partial}{\partial s} \Big|_{r,n} \\ \frac{\partial}{\partial r} \Big|_{s,n} \\ \frac{\partial}{\partial n} \Big|_{s,r} \end{pmatrix} \quad (22)$$

Note that

$$U_\infty \frac{\partial}{\partial x} + w \frac{\partial}{\partial \theta} = W_0(r) \frac{\partial}{\partial s}; \quad W_0(r) \equiv U_\infty \sqrt{1 + (wr/U_\infty)^2} \quad (23)$$

Thus Equation (20) can be written as

$$\begin{aligned} U_\infty W_0 \frac{\partial u}{\partial s} + wr W_0 \frac{\partial w}{\partial s} - a_\infty^2 \operatorname{div} \vec{V} = \\ = -(r-1)(U_\infty u + wrw) \operatorname{div} \vec{V} - 2W_0 \left( u \frac{\partial u}{\partial s} + v \frac{\partial v}{\partial s} + w \frac{\partial w}{\partial s} \right) \end{aligned} \quad (24)$$

where

$$\operatorname{div} \vec{V} = \cos \psi \frac{\partial u}{\partial s} + \sin \psi \frac{\partial w}{\partial s} - \sin \psi \frac{\partial u}{\partial n} + \cos \psi \left( \frac{\partial w}{\partial n} + \frac{\partial v}{\partial r} \Big|_{x,\theta} \right) + \frac{v}{r} \quad (25)$$

Note that the radial derivative has been left untransformed. These equations are now written in terms of velocity components that lie in a surface of constant radius, and are directed along and normal to the free-stream direction:

$$\begin{aligned} u_s = u \cos \psi + w \sin \psi & \quad u = u_s \cos \psi - u_n \sin \psi \\ u_n = -u \sin \psi + w \cos \psi & \quad w = u_s \sin \psi + u_n \cos \psi \end{aligned} \quad (26)$$

It can be shown that

$$\text{div } \vec{V} = \frac{\partial u_s}{\partial s} + \frac{\partial u_n}{\partial n} + \frac{\partial v}{\partial r} \Big|_{x,\theta} + \frac{v}{r}$$

$$U_\infty u + \omega r w = W_0 u_s$$

$$u \frac{\partial u}{\partial s} + w \frac{\partial w}{\partial s} = u_s \frac{\partial u_s}{\partial s} + u_n \frac{\partial u_n}{\partial s} \quad (27)$$

Consequently, the basic differential equation becomes:

$$\begin{aligned} W_0^2 \frac{\partial u_s}{\partial s} - a_\infty^2 \left( \frac{\partial u_s}{\partial s} + \frac{\partial u_n}{\partial n} + \frac{\partial v}{\partial r} \Big|_{x,\theta} + \frac{v}{r} \right) &= \\ = -(\gamma-1) W_0 u_s \left( \frac{\partial u_s}{\partial s} + \cancel{\frac{\partial u_n}{\partial n}} + \cancel{\frac{\partial v}{\partial r}} \Big|_{x,\theta} + \cancel{\frac{v}{r}} \right) & \\ - 2W_0 \left( u_s \frac{\partial u_s}{\partial s} + u_n \cancel{\frac{\partial u_n}{\partial s}} + v \cancel{\frac{\partial v}{\partial s}} \right) & \end{aligned} \quad (28)$$

This equation can be simplified by neglecting the products of disturbance quantities. However, in the transonic range, the quantity  $W_0^2 - a_\infty^2$  is itself a small quantity, which multiplies the term  $\partial u_s / \partial s$ . Thus, the nonlinear terms which contribute to this coefficient are retained, giving

$$\left[ W_0^2 - a_\infty^2 + (\gamma+1) W_0 u_s \right] \frac{\partial u_s}{\partial s} - a_\infty^2 \left[ \frac{\partial u_n}{\partial n} + \frac{\partial v}{\partial r} \Big|_{x,\theta} + \frac{v}{r} \right] = 0 \quad (29)$$

It is significant that, in the small-disturbance approximation, the radial velocity component does not contribute to the transonic nonlinearity.

In addition to  $W_0^2 - a_\infty^2$ , other small parameters related to the blade thickness and loading will play a role in the problem, and an order-of-magnitude analysis is required, to establish the relative magnitudes that may be retained in a consistent analysis. This subject is taken up in Section III.

#### Transonic Shear-Flow Approximation

The similarity of Equation (29) to the conventional two- and three-dimensional rectilinear transonic small-disturbance equations is obvious. However, there are also some very marked differences, which are worthy of further examination, since rectilinear transonic shear flows are sometimes suggested as being

representative of the flow in a transonic compressor blade row.<sup>19-22</sup> The rectilinear equations used in these papers do not contain any of the axisymmetric terms in the divergence of the velocity vector; thus in the small-disturbance limit, their use is tantamount to rewriting Equation (29) as

$$\left[ W_0^2 - a_\infty^2 + (\gamma+1) W_0 u_s \right] \frac{\partial u_s}{\partial s} - a_\infty^2 \left[ \frac{\partial u_n}{\partial n} + \frac{\partial v}{\partial R} \right]_{s,n} = 0 \quad (30)$$

Here  $s$ ,  $R$ , and  $n$  are regarded as rectilinear coordinates, and the approach velocity  $W_0$  is taken to be a linear function of  $R$ , rather than the square-root function corresponding to the resultant of  $U_\infty$  and  $\omega r$ . The correct form of Equation (29) is

$$\left[ W_0^2 - a_\infty^2 + (\gamma+1) W_0 u_s \right] \frac{\partial u_s}{\partial s} - a_\infty^2 \left[ \frac{\partial u_n}{\partial n} + \frac{\partial v}{\partial R} \right]_{s,n} + \frac{\partial v}{\partial s} \frac{\partial s}{\partial r} \bigg|_{x,\theta} + \frac{\partial v}{\partial n} \frac{\partial n}{\partial r} \bigg|_{x,\theta} + \frac{v}{r} = 0 \quad (31)$$

Thus, the rectilinear model can be thought of as neglecting three terms: one of them is the  $v/r$  term, characteristic of the divergence in an axisymmetric flow, while the other two are related directly to the radial variations of the distances measured along and normal to the streamlines.

Moreover, the use of a rectilinear shear flow also introduces a shear disturbance that is not present in the uniform-inlet turbomachinery case. This point is illustrated in the papers of Namba<sup>21</sup> and Inger<sup>22</sup>, which start from the full rectilinear three-dimensional equations, and then proceed to the equations for small disturbances of a transonic shear flow profile. Their equations, for adiabatic flow, show an additional term on the right-hand side of Equation (30), proportional to  $u_n \frac{dW_0}{dr}$ , in addition to the other discrepancies noted above. This additional term does not arise in the present analysis, unless the approach flow  $U_\infty$  itself is taken to vary with  $r$ . The point to be stressed is that the radial velocity variation produced as the resultant of constant vectors  $\vec{U}_\infty$  and  $\vec{\omega}$  is not correctly modeled by a rectilinear shear flow, since small disturbances of the latter flow lead to an equation which differs from the one appropriate to steady flow in blade-fixed coordinates.

#### Velocity-Component Equations

Equation (29) can now be transformed back to the cylindrical coordinates, using:

$$z = \omega x / U_{\infty} \quad , \quad \rho = \omega r / U_{\infty} \quad , \quad M_{\infty} = U_{\infty} / a_{\infty}$$

$$\bar{u} = u / U_{\infty} \quad , \quad \bar{v} = v / U_{\infty} \quad , \quad \bar{w} = w / U_{\infty}$$

$$\frac{\partial}{\partial s} = \frac{U_{\infty}}{w_0} \left( \frac{\partial}{\partial x} + \frac{1}{r} \frac{\partial}{\partial \theta} \right) \quad , \quad \frac{\partial}{\partial r} = \frac{U_{\infty}}{w_0} \left( -\rho \frac{\partial}{\partial x} + \frac{1}{r} \frac{\partial}{\partial \theta} \right)$$

$$u_s = \frac{U_{\infty}}{w_0} (u + \rho w) \quad , \quad u_n = \frac{U_{\infty}}{w_0} (w - \rho u) \quad (32)$$

The result is:

$$\left\{ 1 - M_{\infty}^2 (1 + \rho^2) - (\gamma + 1) M_{\infty}^2 (\bar{u} + \rho \bar{w}) \right\} \left\{ \frac{\partial \bar{u}}{\partial z} + \rho \frac{\partial \bar{w}}{\partial z} + \frac{\partial \bar{u}}{\partial \theta} + \rho \frac{\partial \bar{w}}{\partial \theta} \right\}$$

$$+ \frac{1}{\rho} \frac{\partial \bar{w}}{\partial \theta} - \frac{\partial \bar{u}}{\partial \theta} - \rho \frac{\partial \bar{w}}{\partial z} + \rho^2 \frac{\partial \bar{u}}{\partial z} + (1 + \rho^2) \left( \frac{\partial \bar{v}}{\partial \rho} + \frac{\bar{v}}{\rho} \right) = 0 \quad (33)$$

To this must be added the statement that any two of the three vorticity components are zero:

$$\frac{1}{\rho} \frac{\partial}{\partial \rho} (\rho \bar{w}) = \frac{1}{\rho} \frac{\partial \bar{v}}{\partial \theta} \quad ; \quad \frac{1}{\rho} \frac{\partial \bar{u}}{\partial \theta} = \frac{\partial \bar{w}}{\partial z} \quad ; \quad \frac{\partial \bar{v}}{\partial z} = \frac{\partial \bar{u}}{\partial \theta} \quad (34)$$

#### Potential Equation

The differential equation to be satisfied by the velocity potential can now be found directly from Equation (33). Let  $\Phi$  denote the potential whose gradient gives the dimensional perturbation velocity components; then let dimensionless perturbation quantities be defined as:

$$\phi = \frac{U_{\infty}}{w} \Phi \quad ; \quad \bar{u} = \frac{\partial \Phi}{\partial z} \quad , \quad \bar{v} = \frac{\partial \Phi}{\partial \rho} \quad , \quad \bar{w} = \frac{1}{\rho} \frac{\partial \Phi}{\partial \theta} \quad (35)$$

Then, denoting partial derivatives by subscripts:

$$\left\{ 1 - M_{\infty}^2 (1 + \rho^2) - (\gamma + 1) M_{\infty}^2 (\Phi_z + \Phi_{\theta}) \right\} \left\{ \Phi_{zz} + 2 \Phi_{z\theta} + \Phi_{\theta\theta} \right\}$$

$$+ \rho^2 \Phi_{zz} - 2 \Phi_{z\theta} + \frac{1}{\rho^2} \Phi_{\theta\theta} + (1 + \rho^2) \left( \Phi_{\rho\rho} + \frac{\Phi}{\rho} \right) = 0 \quad (36)$$

The connection between this equation and its linearized counterpart (References 4, 5, 23-29) can be seen by rewriting it as follows, where the nonlinear term has been taken to the right-hand side:

$$\begin{aligned} (1-M_\infty^2) \Phi_{zz} + \Phi_{\rho\rho} + \frac{\Phi_z}{\rho} + \frac{1}{\rho^2} (1-M_\infty^2 \rho^2) \Phi_{\theta\theta} - 2M_\infty^2 \Phi_{\theta z} = \\ = \frac{(\gamma+1)M_\infty^2}{1+\rho^2} (\Phi_z + \Phi_\theta) (\Phi_{zz} + 2\Phi_{z\theta} + \Phi_{\theta\theta}) \end{aligned} \quad (37)$$

Okurounmu and McCune<sup>26</sup> have derived an equation similar to (37), in which the right-hand side is replaced by  $\Lambda (\Phi_z + \Phi_\theta)$ , where  $\Lambda$  is a constant, whose magnitude can be estimated from the rotor geometry and operating conditions.\* Handling of the nonlinear term by the introduction of this constant has been a very useful approximation in the treatment of other transonic-flow problems.<sup>30</sup>

A complete potential equation, in which small disturbances are not assumed, and is not approximated, was presented by Wu (see Reference 15, Equation (26)). It can be checked that the present results are consistent with his.

#### Coordinate Transformation

The cylindrical coordinates  $z, \rho, \theta$  have two features that limit their usefulness for finite-difference evaluations of Equations (33), (34) and (36). The first is that the blade surfaces, where boundary conditions are to be applied, do not lie on constant values of  $z$ ,  $\rho$ , or  $\theta$ . The second is that the axis of the forward Mach cone through any point does not lie parallel to any of these axes. The results of South and Jameson<sup>31</sup> show that unwanted numerical problems may occur when the Mach-cone axes are not nearly aligned with a coordinate direction.

The  $s, r, \eta$  coordinates (Equation (21)) would take care of the latter problem; however, they are not free from the first limitation, because the variation of  $s$  with  $\eta$  causes the blade-surface locations to be a

\* Their result (see Eq. 14, p. 1374 of Ref. 26) does not contain the quantity  $\gamma$  on the right-hand side of Eq. 37, apparently because they neglected the contribution from the term involving  $Q^2 - Q_\infty^2$  in Eq. 20.

complicated function of the radius. Moreover, the fact that the quantities  $\frac{\partial s}{\partial r} \chi, \theta$  and  $\frac{\partial n}{\partial r} \chi, \theta$  in the chain-rule derivatives are nonzero leads to a major increase in the number of terms in the differential equations, especially for the velocity potential.

An alternate set of coordinates that appears to circumvent the limitations cited above is the skew set using the  $\zeta$ -coordinate introduced by Goldstein<sup>32</sup>:

$$\bar{z} = z \quad , \quad \rho = \rho \quad , \quad \zeta = \theta - z \quad (38)$$

In these terms, the velocity-component equations become:

$$\left\{ 1 - M_\infty^2 (1 + \rho^2) - (\gamma + 1) M_\infty^2 (\bar{u} + \rho \bar{w}) \right\} \frac{\partial}{\partial \bar{z}} (\bar{u} + \rho \bar{w}) + \left( \frac{1 + \rho^2}{\rho} \frac{\partial}{\partial \zeta} - \rho \frac{\partial}{\partial \bar{z}} \right) (\bar{w} - \rho \bar{u}) + (1 + \rho^2) \left( \frac{\partial \bar{v}}{\partial \rho} + \frac{\bar{v}}{\rho} \right) = 0 \quad (39)$$

$$\frac{1}{\rho} \frac{\partial}{\partial \rho} (\rho \bar{w}) = \frac{1}{\rho} \frac{\partial \bar{v}}{\partial \zeta} ; \quad \frac{1}{\rho} \frac{\partial \bar{u}}{\partial \zeta} = \frac{\partial \bar{w}}{\partial z} - \frac{\partial \bar{w}}{\partial \zeta} ; \quad \frac{\partial \bar{v}}{\partial z} - \frac{\partial \bar{v}}{\partial \zeta} = \frac{\partial \bar{u}}{\partial \rho} \quad (40)$$

and the velocity potential satisfies:

$$\left\{ 1 - M_\infty^2 (1 + \rho^2) - (\gamma + 1) M_\infty^2 \Phi_{\bar{z}} \right\} \Phi_{\bar{z}\bar{z}} + \rho^2 \Phi_{\bar{z}\bar{z}} - 2(1 + \rho^2) \Phi_{\zeta\bar{z}} + \frac{(1 + \rho^2)^2}{\rho^2} \Phi_{\zeta\zeta} + (1 + \rho^2) \left( \Phi_{\rho\rho} + \frac{1}{\rho} \Phi_\rho \right) = 0 \quad (41)$$

The  $\bar{z}$ -derivatives in this equation are taken at constant  $\zeta$  and  $\rho$ ; thus, they are aligned with the relative freestream velocity vector. The supersonic-propeller studies of Ordway and Hale<sup>33, 34</sup> have shown that the forward Mach cones through any point are centered on the helical streamlines, and are closely approximated by a right circular cone, in the vicinity of the

point. Thus, use of Eq. 41 guarantees the alignment of the Mach-cone axes with lines along which  $\zeta$  and  $\rho$  are constant.

#### Boundary Conditions at the Blade Surfaces

The  $z, \rho, \zeta$  coordinates have the advantage of convenience in expressing the boundary conditions at the blade surfaces. If there are  $B$  blades, whose chord varies with  $r$  in such a way as to have a constant axial projection  $C_a$ , then they are located at

$$\zeta = \frac{2j\pi}{B}, \quad j = 0, 1, 2, \dots, B-1; \quad 0 \leq z \leq \frac{\omega C_a}{U_\infty} \quad (42)$$

The conditions prescribed at the blades will involve either the blade shape or the local pressure; these are related to the velocities by (see Reference 5, p. 9):

$$\frac{u_n}{w_0} = \frac{\alpha n}{\alpha s} \quad \text{or} \quad -2 \left( \frac{w_0}{U_\infty} \right)^2 \frac{u_s}{w_0} = \frac{\int - \int \omega}{\frac{1}{2} \rho_\infty U_\infty^2} \quad (43)$$

(Here  $\rho_\infty$  denotes the density far upstream). The quantities  $u_s$  and  $u_n$  are related to the other velocity components and the potential by:

$$\frac{u_n}{w_0} = \left( \frac{U_\infty}{w_0} \right)^2 (\bar{w} - \rho \bar{u}) = \frac{-\rho^2 \Phi_{z\theta} + \Phi_{\theta z}}{\rho(1+\rho^2)} = \frac{1}{\rho} \Phi_{\zeta z} - \frac{\rho}{1+\rho^2} \Phi_{z\zeta} \quad (44)$$

$$\frac{u_s}{w_0} = \left( \frac{U_\infty}{w_0} \right)^2 (\bar{u} + \rho \bar{w}) = \frac{\Phi_{z\theta} + \Phi_{\theta z}}{1+\rho^2} = \frac{\Phi_{z\zeta}}{1+\rho^2}$$

These perturbation quantities will appear in the boundary conditions in various combinations, depending on how the problem is posed. There are at least three cases of interest:

1.) The first case might be referred to as the "off-design" condition. In it, the entire blade shape is given in terms of the camberline and thickness distributions,  $h(s)$  and  $t(s)$  respectively:

$$\eta_{uL}(s) = h(s) \pm t(s)/2 \quad (45)$$

$$h(s) = (\eta_u + \eta_L)/2 ; t(s) = \eta_u - \eta_L$$

2.) In the second case, which might be called the "design" condition, the blade thickness distribution  $t(s)$  and the loading distribution on the blade  $p_L(s) - p_u(s)$  are given. Thus, the boundary conditions will involve  $u_\eta$ , and differences of  $u_s$  across the blade surface.

3.) A third case of interest is that in which the pressure distributions on upper and lower surfaces,  $p_u(s)$  and  $p_L(s)$ , are specified (as might be dictated by boundary-layer growth considerations, for example). The problem is then to determine the corresponding blade shape. This case amounts to a specification of  $u_s$  on each blade surface.

In all of the above cases, the boundary conditions are applied on the line  $\zeta = 2i\pi/\beta$ , rather than at the blade surfaces. This linearization of the boundary conditions is consistent with the order retained in the differential equations.

At the hub ( $\rho = \rho_h$ ) and at the casing ( $\rho = \rho_r$ ), the radial velocity is proportional to the streamwise slope of the hub and casing surfaces. In the present work, these surfaces are assumed to be cylindrical; thus, the radial velocities at these walls are zero:

$$\Phi_\rho(\rho_h) = \Phi_\rho(\rho_r) = 0 \quad (46)$$

### Periodicity and Farfield Conditions

The flowfield must be periodic in the  $\theta$ -direction at fixed  $z$ , with period  $2\pi/B$ . Thus the perturbation quantities, such as velocity components and pressure, must display this periodicity. However, it is not necessary that the velocity potential be periodic.

In an analytic solution that is constructed by an eigenfunction expansion, it is easy to satisfy the periodicity requirement by proper choice of the eigenfunctions. For the present considerations, which are directed at numerical solutions, this procedure is not available. However, an alternate procedure that appears to be suited to the mixed elliptic/hyperbolic nature of the problem is to require that the perturbation velocities  $u_3$  and  $u_\eta$  be periodic on the helical surfaces in which the blades lie, i.e.,

$$\begin{aligned}\phi_z(z, \rho, 2\pi/B) &= \phi_z(z, \rho, 0) \\ \phi_s(z, \rho, 2\pi/B) &= \phi_s(z, \rho, 0)\end{aligned}\tag{47}$$

It is not required that the radial perturbation velocity or the potential be periodic on these surfaces. In fact, vortex sheets will in general trail downstream of the blade surfaces, and both the potential and radial velocity will be discontinuous across these surfaces.

The perturbation potential is defined to be zero far upstream; thus at any point along the helical surfaces that contain the blades, the potential is given by

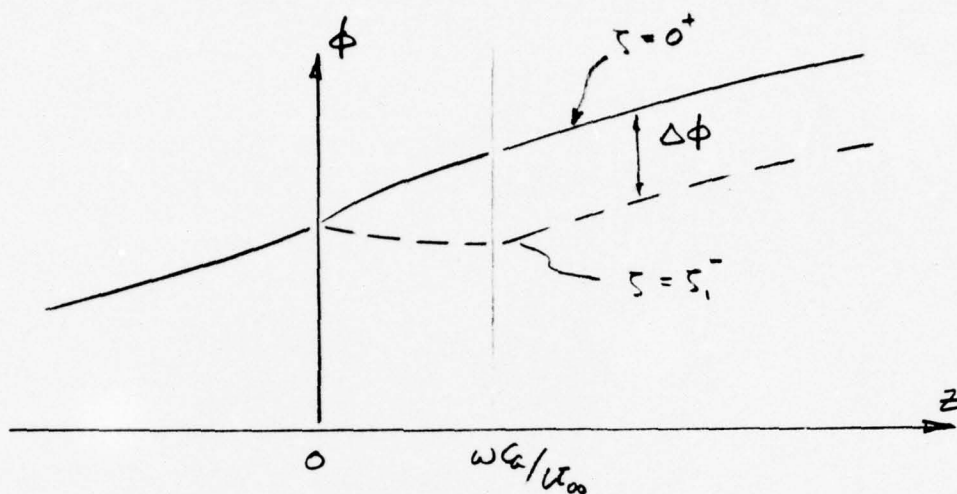
$$\begin{aligned}\phi(z, \rho, \sigma^+) &= \int_{-\infty}^z \phi_z(z, \rho, \sigma^+) dz \\ \phi(z, \rho, \sigma^-) &= \int_{-\infty}^z \phi_z(z, \rho, \sigma^-) dz\end{aligned}\tag{48}$$

where  $\sigma_i = 2\pi/B$ . Since the integrands are periodic upstream of the blades, it follows that  $\phi$  itself is also periodic there:

$$\phi(z, \rho, \sigma_i^-) = \phi(z, \rho, \sigma_i^+), \quad -\infty \leq z \leq 0\tag{49}$$

If the integration is now extended onto the blades, the results will in general be different, until the trailing edge is reached; the potential difference

existing there will remain unchanged downstream:



$$\phi(z, \rho, \sigma^+) - \phi(z, \rho, \sigma_1^-) = \Delta\phi(\rho), \quad \frac{\omega Ca}{U_\infty} \leq z \leq \infty \quad (50)$$

This jump in potential is proportional to the normal force per unit span  $dN/dr$ ; by integrating the pressure difference (pressure side minus suction side) along the blade at constant radius, it is found that

$$\sqrt{1+\rho^2} \Delta\phi(\rho) = \frac{\omega}{U_\infty} \frac{dN}{dr} / \frac{1}{2} \rho_\infty U_\infty^2 \quad (51)$$

The jump in potential is also related to the mean turning angle downstream of the blades

$$\omega_{avg} = \frac{U_\infty}{\rho \sigma_1} \int_0^{\sigma_1} \phi_\sigma d\sigma = - \frac{U_\infty B}{2\pi \rho} \Delta\phi(\rho) \quad (52)$$

In addition, the jump in potential is related to the total pressure ratio across the blade row. In the full nonlinear treatment<sup>17</sup>, this quantity

is found from the stagnation temperature ratio

$$\frac{p_{02}}{p_{01}} = \left( \frac{T_{02}}{T_{01}} \right)^{\gamma/(\gamma-1)}$$

which in turn is given by the relation:

$$C_p (T_{02} - T_{01}) = \omega (r_2 V_{\theta 2} - r_1 V_{\theta 1})$$

Here the subscripts 1 and 2 refer to stations upstream and downstream of the blades. In the present notation,

$$V_{\theta} = \omega r - \omega r = \omega$$

If the mean value calculated above is used for  $\omega$ , if  $T_{01}$  is expressed in terms of the inlet Mach number, and if streamline deflections  $r_2 - r_1$  are neglected, then the leading term in the expression for the total pressure ratio is

$$\frac{p_{02}}{p_{01}} = 1 + \frac{\gamma M_{\infty}^2}{1 + \frac{\gamma-1}{2} M_{\infty}^2} \cdot \frac{B}{2\pi} \Delta\phi(r) \quad (53)$$

The vortex sheets that trail downstream of the blades are assumed to lie in the helical surfaces. The jump in potential across this surface must be taken into account when making finite-difference approximations to derivatives near the sheet. One of the manifestations of this problem involves the evaluation of  $\phi_{\zeta\zeta}$ . Following the procedure outlined by Ballhaus and Bailey<sup>12</sup>, the potential is divided into odd and even parts:

$$\phi = \phi^o + \phi^e$$

where

$$\begin{aligned} \phi^e(z, \rho, \zeta) &= \frac{1}{2} \left\{ \phi(z, \rho, \zeta - \zeta_1) + \phi(z, \rho, \zeta_1 - \zeta) \right\} \\ \phi^o(z, \rho, \zeta) &= \frac{1}{2} \left\{ \phi(z, \rho, \zeta - \zeta_1) - \phi(z, \rho, \zeta_1 - \zeta) \right\} \end{aligned}$$

Along  $\zeta = \zeta_1^-$ , the quantity  $\phi_z^o$  is zero, because  $\Delta\phi$  is independent of  $z$ ; thus by differentiation,  $\phi_{zz}^o$  is also zero there. Across  $\zeta = \zeta_1$ ,  $u_n$  and  $u_s$  are continuous, hence  $\phi_z$  and  $\phi_\zeta$  are continuous also. Thus  $\phi_{\zeta z}^o$  is zero on  $\zeta = \zeta_1^-$ , which says that the entire variation of  $\phi_{\zeta z}$  is in the even part.

Consequently, along  $\zeta = \zeta_1^-$ , the even part of  $\phi$  satisfies the original partial differential equation, and can be differenced in a straightforward manner, while the odd part satisfies

$$\frac{1+\rho^2}{\rho^2} \phi_{\zeta\zeta}^0 + \phi_{\rho\rho}^0 + \frac{1}{\rho} \phi_{\rho}^0 = 0$$

But it is also true that  $\phi^0(z, \rho, \zeta_1^{\pm}) = \pm \frac{1}{2} \Delta\phi$ . Thus the odd part of  $\phi_{\zeta\zeta}^0$  is found by a finite-difference approximation of

$$\phi_{\zeta\zeta}^0(z, \rho, \zeta_1^{\pm}) = \pm \frac{\rho^2}{2(1+\rho^2)} \left\{ (\Delta\phi)_{\rho\rho} + \frac{1}{\rho} (\Delta\phi)_{\rho} \right\} \quad (54)$$

### Farfield Conditions

At large distances downstream of the blade row, the perturbation velocities must not change along the helical directions, i.e., there must be no variation with  $z$  at constant  $\rho$  and  $\zeta$ :

$$\lim_{z \rightarrow \infty} \frac{\partial}{\partial z} \{ \bar{u}, \bar{v}, \bar{w} \}_{\rho, \zeta} = 0$$

Thus the perturbation potential must be of the form

$$\lim_{z \rightarrow \infty} \phi(z, \rho, \zeta) = f(\rho, \zeta) + Cz \quad (55)$$

The value of the second term can be found by the requirement of mass conservation:

$$\dot{m} = \rho_{\infty} U_{\infty} \pi (r_T^2 - r_H^2) = \int_{r_H}^{r_T} \int_0^{2\pi} \rho w_x r dr d\theta$$

If the density and axial velocity are expanded to first order in the perturbation velocities, the expression for the corresponding mass-flow perturbation, which must be zero, is:

$$\int_{r_H}^{r_T} \int_0^{2\pi/B} \left\{ (1-M_{\infty}^2) \bar{u} - \rho M_{\infty}^2 \bar{w} \right\} \rho dr d\zeta = 0$$

The integral involving  $\bar{w}$  is related to  $\Delta\phi$  (see Eq. 52), and the quantity  $\bar{u} + \rho\bar{w}$  is equal to the constant  $C$ , which can be solved for as

$$C = \frac{-B}{\pi (1-M_{\infty}^2) (\rho_T^2 - \rho_H^2)} \int_{\rho_H}^{\rho_T} \rho \Delta\phi d\rho \quad (56)$$

This constant is proportional to the static pressure rise through the blade row, as noted by Okorounum and McCune.<sup>25</sup>

Finally, a Kutta condition must be imposed at the trailing edges of the blades. In a full nonlinear treatment, this would require that a stagnation point be located at a rounded trailing edge or at a trailing edge having a non-zero wedge angle, and, at a cusped trailing edge, would require that the pressure be continuous across the trailing edge. In the small-disturbance approximation, it is not possible to represent a stagnation point, and thus, the solution becomes singular at the trailing edge. The finite-difference evaluation of the solution smoothes out this singular behavior, replacing it with finite values of the velocity components. In the present work, the circulation  $\Delta\phi$  is adjusted until the pressures corresponding to these finite velocity components are continuous across the trailing edge.

### III. SIMILARITY PARAMETERS

The equations presented in the previous section contain the leading nonlinear terms that must be retained when the difference of the relative Mach number from one is small. The specific combination of terms retained implies an assumption that

$$\frac{u_s}{w_0} = O(1 - M_0^2)$$

However, the boundary conditions imposed at the blade surfaces also require that  $u_s$  and  $u_n$ , or some combination of them, will have orders of magnitude that are dictated by the small parameters that measure the blade geometry and loading. Because these components are connected by the equations of motion, the small parameters must then be related to each other, in order that the equations be consistently ordered in the limit where these parameters approach zero. This section contains a discussion of the geometric and loading parameters, and their relation to  $1 - M_0^2$  in the small-disturbance limit.

The blade thickness and lift distributions are taken to be characterized by the small parameters  $\tau$  and  $\alpha$ , where  $\tau/\alpha = O(1)$ . These parameters directly affect the orders of the velocity components  $u_s$  and  $u_n$ , in a manner discussed below. The order of the radial component,  $v$ , is affected only indirectly by the parameters  $\tau$  and  $\alpha$ , in the sense that the continuity requirements will cause the radial velocity component to respond to the perturbations in the other two components. In a properly designed blade row, this overall continuity requirement is reflected in an axial rate of change of the annular cross section, whose magnitude is influenced by the thickness and loading parameters. For the purposes of the present analysis, the rate of change of the annular cross-sectional area is not introduced explicitly as a small parameter. Rather, the radial perturbation velocity is carried along in the equations, with a view to relating its order, through the other two components, to the thickness and loading parameters. Thus, the basic ordering problem is treated in a quasi two-dimensional manner, involving only  $u_s$  and  $u_n$ .

The appropriate equations are Equation (28) and the first component of the irrotationality condition, here rewritten with the  $s$ - and  $n$ -coordinates made dimensionless by the local chord length

$$\begin{aligned} \left\{ 1 - M_0^2 - (\gamma + 1) M_0^2 \frac{u_s}{w_0} \right\} \frac{\partial(u_s/w_0)}{\partial(s/c)} + \frac{\partial(u_n/w_0)}{\partial(n/c)} + \frac{c}{r} \frac{\partial\left(\frac{r}{c} \frac{v}{w_0}\right)}{\partial(r/c)} \\ = (\gamma - 1) M_0^2 \frac{u_s}{w_0} \frac{\partial(u_n/w_0)}{\partial(n/c)} + 2 M_0^2 \frac{u_n}{w_0} \frac{\partial(u_n/w_0)}{\partial(s/c)} \\ \frac{\partial(u_s/w_0)}{\partial(n/c)} = \frac{\partial(u_n/w_0)}{\partial(s/c)} \end{aligned} \quad (57)$$

The next step is to establish the dependence of the velocity components on the parameter  $\tau$ . This dependence is influenced by the solidity of the blade row,  $c/L_T$ . At very low solidity, the dependence approaches that of the isolated airfoil case. This can be seen by examining the blade-surface boundary condition, i.e.,

$$\frac{u_n}{w_0} = \frac{d\eta}{ds} = \tau g'(s/c) \quad (58)$$

where  $g$  is of unit order. If the equations above are divided by  $\beta_0^4$  and  $\beta_0^3$ , respectively, where  $\beta_0^2 = 1 - M_0^2$ , it follows that the solution has the familiar transonic similitude:

$$\frac{u_s/w_0}{\beta_0^2}, \frac{u_n/w_0}{\beta_0^3} = f_{\text{ens}}\left(\frac{s}{c}, \frac{\beta_0 \tau}{c}; K\right) \quad (59)$$

where

$$K \equiv \frac{[(\gamma + 1) M_0^2 \tau]^{2/3}}{1 - M_0^2} = O(1) \quad (60)$$

and where all the arguments appearing in the functions are of unit order. The dependences of  $u_s$  and  $u_n$  display the well-known tendency of disturbances in two-dimensional transonic flows to be felt at large transverse distances. The full implications of this similitude have been studied, both theoretically and experimentally, by Amecke.<sup>35</sup>

The requirement that  $\beta_0^{1/2}$  be of unit order cannot be satisfied if the solidity becomes of unit order, since then  $\eta/c$  is restricted to values of order one, while  $\beta_0 \rightarrow 0$ . In this range, a new phenomenon comes into play, namely that the flow between the blades begins to act like a transonic channel flow, in which the distance over which the transition through sonic conditions occurs is controlled by the effective radius of curvature of the channel. This influence was first pointed out by Ackeret and Rott<sup>36</sup>. The implications on the ordering of the flow variables has been studied by Hall<sup>37</sup>, who observed that the axial extent of the transonic zone (which affects the ordering of the streamwise coordinate) is governed by the radius of curvature of the channel throat.

The adaptation of Hall's analysis to the present problem leads to the following conclusions. The normal velocity component at the blade surface is still given by Equation (58), but it is no longer true that  $u_n/w_0$  is of order  $\epsilon$ , since the surface slope function itself vanishes at the sonic location. In order to establish the orders, it is necessary to use the irrotationality condition:

$$\left. \frac{\partial (u_s/w_0)}{\partial (\eta/c)} \right|_{\eta=0} = \left. \frac{\partial (u_n/w_0)}{\partial (s/c)} \right|_{\eta=0} = \tau q''(s/c) \quad (61)$$

where surface curvature  $q''(s/c)$  is of unit order, and does not vanish in the region of near-sonic flow. Since  $\eta/c = O(1)$ , it can be concluded that  $u_s/w_0 = O(\epsilon)$ . In order to deduce the orders of  $u_n/w_0$  and  $s/c$ , Equation (57) is differentiated with respect to  $s/c$ , and the irrotationality condition is used to eliminate  $u_n$ :

$$\left[ \beta_0^2 - (\gamma+1)M_0^2 \frac{u_s}{w_0} \right] \frac{\partial^2 (u_s/w_0)}{\partial (s/c)^2} + \frac{\partial^2 (u_s/w_0)}{\partial (\eta/c)^2} = O \left( \frac{\partial (u_s/w_0)}{\partial (s/c)} \right)^2 \quad (62)$$

From the known orders of  $u_s/N_0$  and  $v/c$ , it is clear that we must have

$$\beta_0^2 = O(\tau), \quad \frac{s}{c} = O(\tau^{1/2})$$

The solution is then of the form

$$\frac{u_s/N_0}{\tau}, \quad \frac{v/c}{\tau^{3/2}} = f_{\text{ens}} \left( \frac{s}{c\tau}, \frac{v}{c}; \frac{\beta_0^2}{\tau}, \frac{\alpha}{\tau}, \frac{c}{L} \right) \quad (63)$$

where all of the parameters are of unit order. It can now be verified that the nonlinear terms on the right-hand side of Equation (62) are smaller by a factor  $\tau$  than those retained.

It should be noted that the similarity parameter  $\tau/\beta_0^2$  appears in a number of papers that deal with transonic channel flow. As an example, it is the appropriate parameter in the low-frequency limit of Adamson's study of time-dependent transonic channel flow.<sup>38</sup>

The orders of magnitude of the radial velocity and the radial coordinate can now be related to those found above, by using the two components of the irrotationality condition in which  $v$  appears. The result, for any value of the solidity, is that  $v$  and  $r$  take on the same orders as those of  $u_n$  and  $v$ . Thus, the terms in the small-disturbance nonlinear potential equation that permit radial communication may be retained, in a consistent ordering scheme.

It should be stressed that the order-of-magnitude analysis above is only aimed at assuring the consistency of the potential equation derived earlier, which is used here in the sense of a composite equation. It is not intended to be a definitive similitude study. Because of the complexity of the problem, and the large number of parameters present, it is likely that further analysis will lead to more precise definitions of similarity parameters, and to more refined approximations that may be used in the appropriate ranges of these parameters. Similitude studies of three-dimensional flows over isolated wings and bodies have yielded a wide variety of such parameters.<sup>39</sup> It seems probable that a comparable variety remains to be found for three-dimensional turbo-machinery flows.

## CONCLUDING REMARKS

The derivation of the small-disturbance equations presented above is the first step in a study of the combined effects of three-dimensionality and nonlinearity in the transonic flow through a compressor blade row. The high degree of similarity between these equations and those appropriate to isolated airfoils in transonic flow suggests that many of the numerical techniques developed for calculating the latter flows can be carried over to the case of turbomachinery flows. This carryover requires certain adaptations, to account for the periodicity conditions and the somewhat different statement of the blade-surface boundary conditions. These adaptations have been made successfully, and are reported in Reference 40. The fact that these adaptations can be made for the small-disturbance equations, suggests that it should be a relatively straightforward matter to extend the adaptations farther into the nonlinear range.

The equations derived above are also useful in assessing the approximations inherent in the use of a rectilinear shear flow as a model of a compressor flow. There are significant differences between these models and the equations appropriate to a blade row, especially in regard to the representation of three-dimensional effects. Fortunately, the equations derived here appear to be no more complicated than these qualitative models.

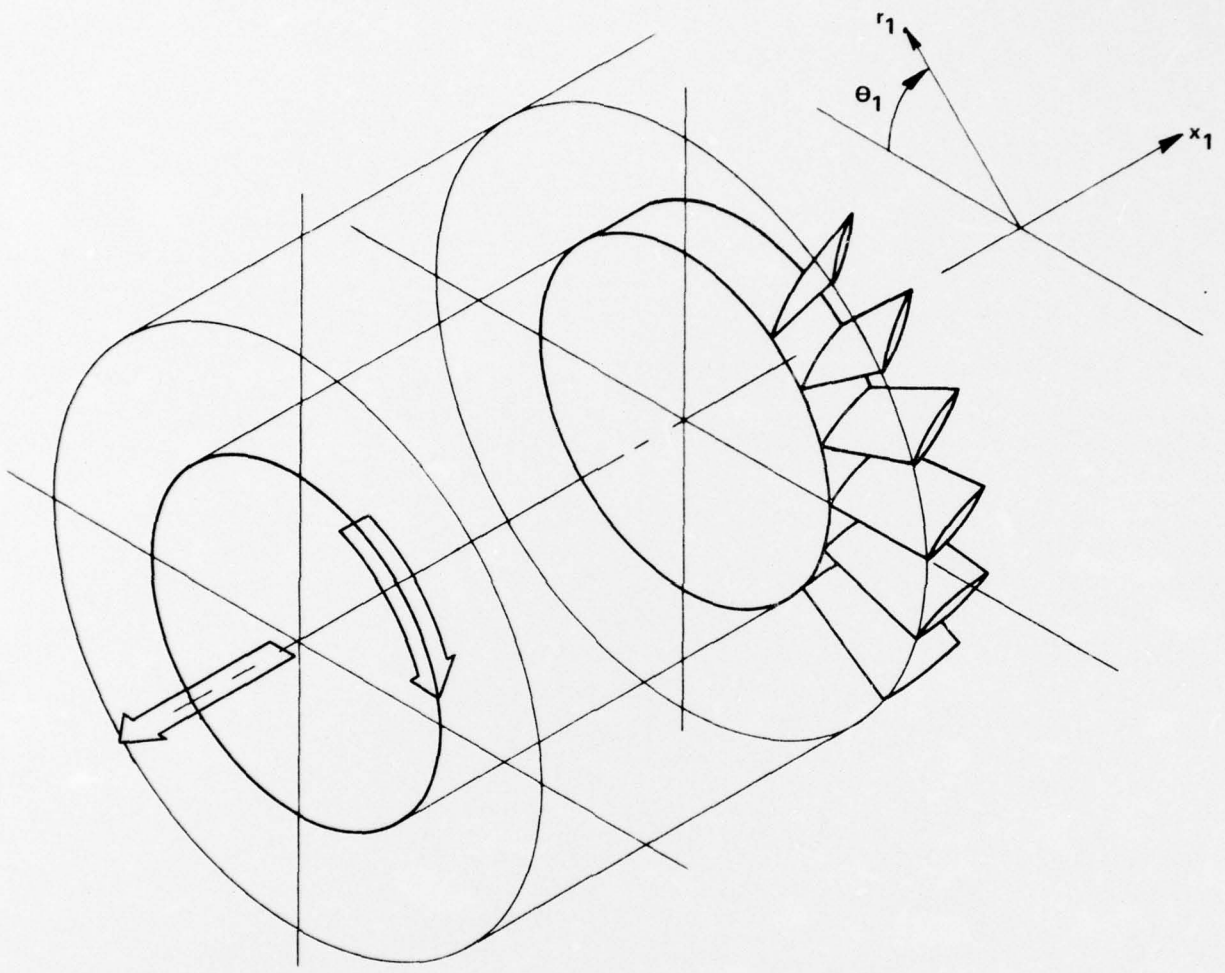


Figure 1 SPACE FIXED COORDINATES  
ROTOR ADVANCES AND ROTATES  
IN AIR AT REST

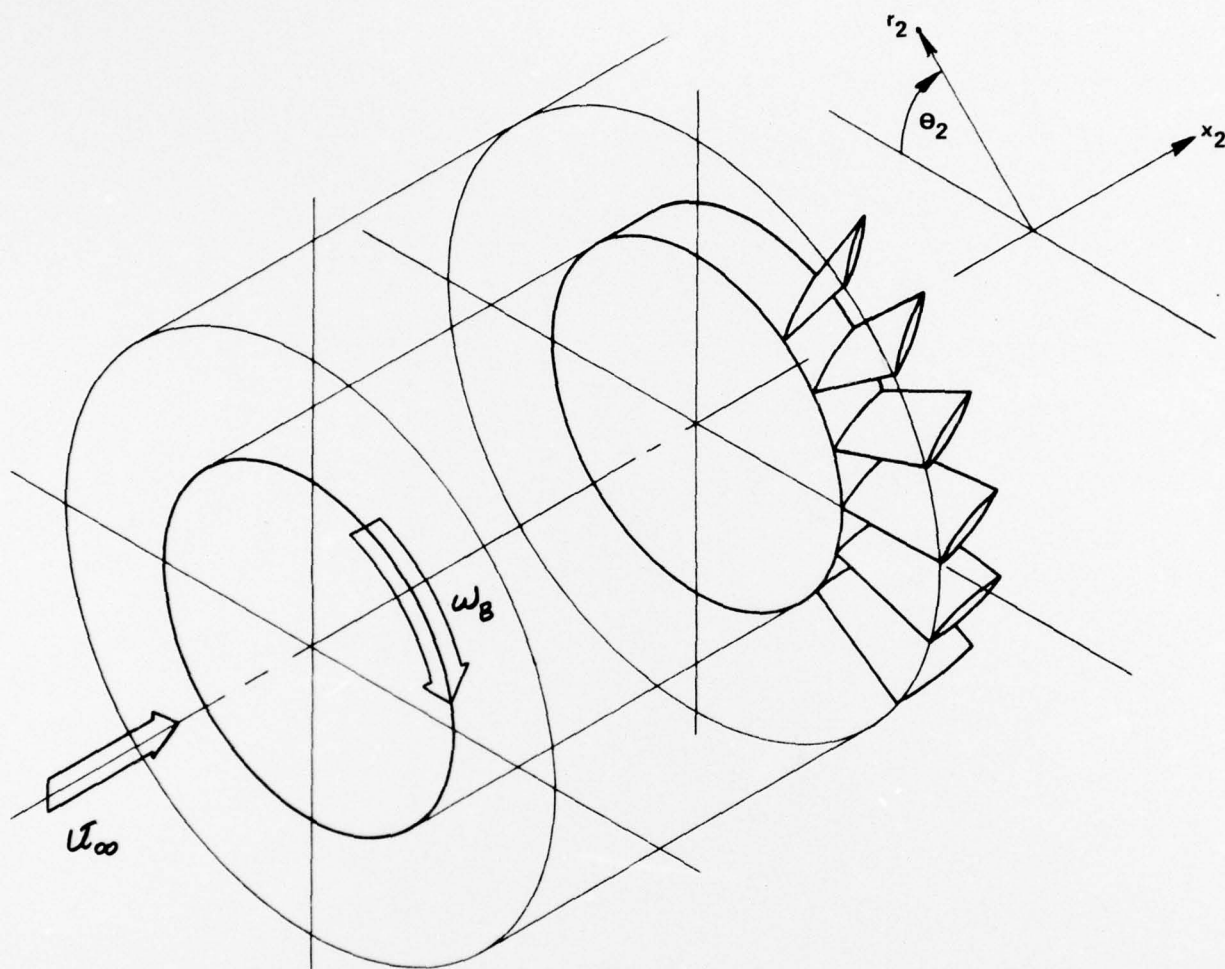


Figure 2 ABSOLUTE COORDINATES  
 ROTOR ROTATES IN AN AXIAL FLOW

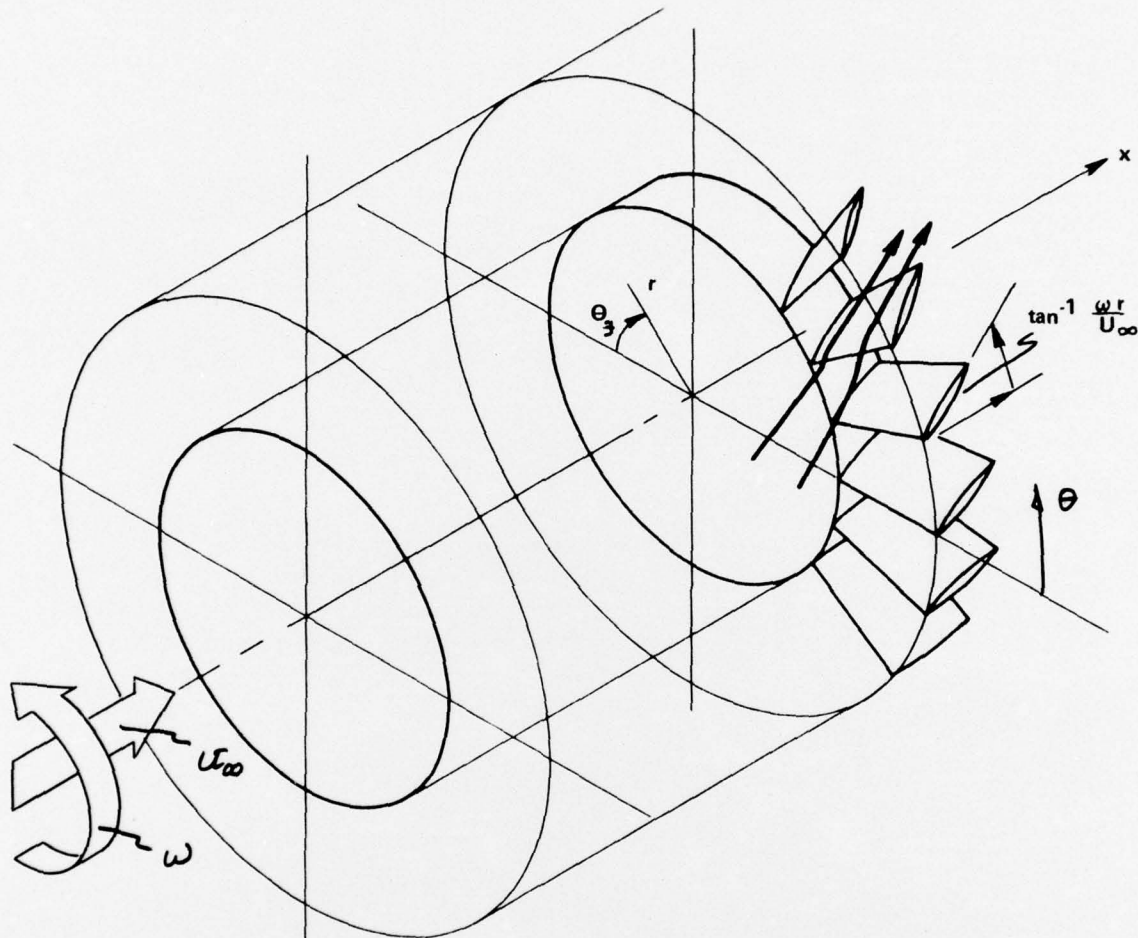


Figure 3 BLADE-FIXED COORDINATES  
 ROTOR IS STATIONARY IN A  
 HELICAL APPROACH FLOW

## REFERENCES

1. Hartmann, M. J., Benser, W. A., Hauser, C. H. and Ruggeri, R. S. "Fan and Compressor Technology", pp. 1-36 of Aircraft Propulsion, proceedings of a conference held at NASA Lewis Research Center, November 18-19, 1970, NASA SP-259, 1971.
2. Katsanis, T. "Computer Program for Calculating Velocities and Streamlines on a Blade-to-Blade Stream Surface of a Turbomachine", NASA TN D-4525, April 1968.
3. Kurzrock, J. W. and Novick, A. S. "Transonic Flow Around Compressor Rotor Blade Elements. Volume I: Analysis", Air Force Aero Propulsion Laboratory Report, AFAPL TR-73-69, August 1973.
4. McCune, J. E. "The Transonic Flow Field of an Axial Compressor Blade Row", Journal of the Aerospace Sciences, Vol. 25, No. 10, October 1958, pp. 616-626.
5. Erickson, J. C., Lordi, J. A., and Rae, W. J. "On the Transonic Aerodynamics of a Compressor Blade Row", Calspan Corporation Report AI-3003-A-1, October 1971.
6. Benser, W. A., Bailey, E. E., and Gelder, T. F. "Holographic Studies of Shock Waves Within Transonic Fan Rotors", Paper presented at the ASME Nineteenth International Gas Turbine Conference, Zurich, Switzerland, March 30 - April 4, 1974. Available as NASA TM X-71430.
7. Krupp, J. A., "The Numerical Calculation of Plane Steady Transonic Flows Past Thin Lifting Airfoils", Boeing Scientific Research Laboratories Report D180-12958-1, June 1971.
8. Murman, E. M., and Cole, J. D., "Calculation of Plane Steady Transonic Flows", AIAA Journal 9, 1971, pp. 114-121.
9. Murman, E. M., and Krupp, J. A., "Solution of the Transonic Potential Equation Using a Mixed Finite Difference System", Proceedings of the Second International Conference on Numerical Methods in Fluid Dynamics, published as Vol. 8 of Lecture Notes in Physics, Springer-Verlag, 1971, pp. 199-206.
10. Krupp, J. A., and Murman, E. M., "Computation of Transonic Flows Past Lifting Airfoils and Slender Bodies", AIAA Journal 10, 1972, pp. 880-886.
11. Bailey, F. R., and Steger, J. L., "Relation Techniques for Three-Dimensional Transonic Flow about Wings", AIAA Journal 11, (March 1973) pp. 318-325.

12. Ballhaus, W.F., and Bailey, F.R., "Numerical Calculation of Transonic Flow about Swept Wings", AIAA Paper 72-677, June 1972.
13. Steger, J.L. and Klineberg, J.M., "A Finite-Difference Method for Transonic Airfoil Design", AIAA Journal, 11 (May 1973) 628-635.
14. Jameson, A., "Numerical Calculation of the Three-Dimensional Transonic Flow over a Yawed Wing", Proceedings of the AIAA Computational Fluid Dynamics Conference (July 1973), pp. 18-26.
15. Wu, Chung-Hua, "A General Theory of Three-Dimensional Flow in Subsonic and Supersonic Turbomachines of Axial-, Radial-, and Mixed-Flow types", NASA TN 2604, January 1952.
16. Vavra, M.H., Aero-Thermodynamics and Flow in Turbomachines, Wiley & Sons, New York, 1960.
17. Johnsen, I.A. and Bullock, R.O., eds. Aerodynamic Design of Axial-Flow Compressors, NASA SP-36, 1965.
18. Kerrebrock, J.L., "Waves and Wakes in Turbomachine Annuli with Swirl", AIAA Paper 74-87 (1974).
19. Oliver, D.A. and Sparis, P., "Computational Studies of Three-Dimensional Transonic Shear Flow: Work in Progress", NASA CR-1816, May 1971.
20. Oliver, D.A. and Sparis, P., "A Computational Study of Three-Dimensional Transonic Shear Flow in Turbomachine Cascades", AIAA Paper 71-83, January 1971.
21. Namba, M., "Theory of Transonic Shear Flow Past a Thin Aerofoil", J. Fluid Mech. 36 (1969) 759-783.
22. Inger, G.R. and Mason, W.H., "Inviscid Small Disturbance Theory for Nonuniform Transonic Flows", College of Engineering, Virginia Polytechnic Institute and State University, Report VPI-E-73-14, May 1973.
23. McCune, J.W., "The Three-Dimensional Flow Field of an Axial Compressor Blade Row - Subsonic, Transonic, and Supersonic", Ph.D. Thesis, Cornell University, February 1958.
24. McCune, J.E., "A Three-Dimensional Theory of Axial Compressor Blade Rows - Application in Subsonic and Supersonic Flows", Journal of the Aerospace Sciences, Vol. 25, No. 9, September 1958, pp. 544-560.
25. Okurounmu, O. and McCune, J.E., "Three-Dimensional Vortex Theory of Axial Compressor Blade Rows at Subsonic and Transonic Speeds", AIAA Journal, Vol. 8, No. 7, July 1970, pp. 1275-1283.

26. Okurounmu, O. and McCune, J.W., "Lifting Surface Theory of Axial Compressor Blade Rows: Part I - Subsonic Compressor, Part II - Transonic Compressor", AIAA Journal 12, (October 1974), 1363-1380.
27. Lordi, J.A., "Report on a Study of Noise Generation by a Rotating Blade Row in an Infinite Annulus", U.S. Air Force Office of Scientific Research Scientific Report AFOSR TR-71-1485 (also available as Calspan Corporation Report AI-2836-A-1), May 1971.
28. Lordi, J.A., "Noise Generation by a Rotating Blade Row in an Infinite Annulus", AIAA Paper No. 71-617, AIAA 4th Fluid and Plasma Dynamics Conference, Palo Alto, California, June 21-23, 1971.
29. Lordi, J.A., Homicz, G.F. and Rehm, R.G., "Theoretical Studies on Fan Noise Generation by a Transonic Compressor Blade Row", Calspan Corporation Report AI-2836-A-2, August 1973.
30. Oswatitsch, K., "Flow Around Bodies of Revolution at Mach Number One", Proceeding of the Conference on High Speed Aerodynamics, Polytechnic Institute of Brooklyn (January 1955), pp. 113-131.
31. South, J.C. and Jameson, A., "Relaxation Solutions for Inviscid Axisymmetric Transonic Flow over Blunt or Pointed Bodies", pp. 8-17 of Proceedings of the AIAA Computational Fluid Dynamics Conference July 1973.
32. Goldstein, S., "On the Vortex Theory of Screw Propellers", Proc. Roy. Soc., A123, 444 (1929).
33. Ordway, D.E., "An Aerodynamic Theory of a Supersonic Propeller", Ph.D. Thesis, Cornell University, June 1956.
34. Ordway, D.E. and Hale, R.W., "Theory of Supersonic-Propeller Aerodynamics", Journal of the Aero/Space Sciences, Vol. 27, No. 6, June 1960, pp. 437-451.
35. Amecke, J., "Anwendung der Transsonischen Ahnlichkeitsregel auf die Stromung durch Ebene Schaufelgitter", Deutsche Gesellschaft fur Luft - und Raumfahrt, Jahrestagung, (September 1969) Paper 24, AIAA Technical Information Service, A70-15183.
36. Ackeret, J and Rott, N., "Ueber die Stromungen von Gasen durch ungestaffelte Profilgitter", Schweizerische Bauzeitung, 67, (1949), pp. 40-41, 58-61.
37. Hall, I.M., "Transonic Flow in Two-Dimensional and Axially Symmetric Nozzles", Quarterly Journal of Mechanics and Applied Mathematics, 15 (1962), 487-508.

38. Adamson, T.C., "Unsteady Transonic Flows in Two-Dimensional Channels", *Journal of Fluid Mechanics* 52 (1972) 437-449.
39. Cheng, H.K. and Hafez, M.M., "Transonic Equivalence Rule: A Non-linear Problem Involving Lift", *Journal of Fluid Mechanics*, 72 (1975), pp. 161-188.
40. Rae, W.J. "Relaxation Solutions for Three-Dimensional Transonic Flow Through a Compressor Blade Row, The Nonlinear Small-Disturbance Approximation" Calspan Corporation Report No. AB-5487-A-2, (August 1976).

DISTRIBUTION LIST FOR CALSPAN REPORT NO. AB-5487-A-1

Prof. Douglas E. Abbott  
Purdue University  
Thermal Sciences & Propulsion Center  
West Lafayette, IN 47907

Dr. John Adamczyk  
NASA Lewis Research Center  
Cleveland, OH 44135

Dr. Thomas C. Adamson  
College of Engineering  
University of Michigan  
Ann Arbor, MI 48105

Dr. Robert A. Arnoldi  
United Technologies Corporation  
Pratt & Whitney Aircraft Division  
400 Main Street  
East Hartford, CT 06108

Dr. Hafiz Atassi  
University of Notre Dame  
Department of Aerospace &  
Mechanical Engineering  
Notre Dame, IN 46556

Dr. F. R. Bailey  
NASA Ames Research Center  
Moffett Field, CA 94035

Dr. William Ballhaus  
NASA Ames Research Center  
Moffett Field, CA 94035

Prof. J. Chauvin  
von Karman Institute  
Rhode-Saint-Genese  
Belgium

Prof. H. K. Cheng  
School of Engineering  
University of Southern California  
Los Angeles, CA 90007

Dr. Julian Cole  
University of California at Los Angeles  
Los Angeles, CA 90024

Mr. Paul R. Dodge  
AiResearch Manufacturing Company  
Division of Garrett Corporation  
402 So. 36th Street  
Phoenix, AZ 85034

Dr. John Erdos  
General Applied Science Laboratories  
Westbury, NY 11590

Dr. J. C. Evvard  
RFD 5, Box 127  
Laconia, NH 03246

Mr. J. Fabri  
ONERA  
Chatillons-sous-Bagneux  
92320 Chatillon  
France

Dr. S. Fleeter  
Detroit Diesel Allison  
Indianapolis, IN 46206

Dr. Anthony A. Ganz  
Pratt & Whitney Aircraft  
400 Main Street  
East Hartford, CT 06108

Dr. Wayland C. Griffith  
North Carolina State University  
School of Engineering  
Raleigh, NC 27607

Dr. J. Gordon Hall  
Department of Mechanical Engineering  
State University of New York  
at Buffalo  
Buffalo, NY 14214

Dr. Wesley L. Harris  
Massachusetts Institute of Technology  
Cambridge, MA 02139

Prof. A. Hamed  
University of Cincinnati  
Cincinnati, OH 45221

Dr. G. David Huffman  
Indianapolis Center for  
Advanced Research  
1300 West Michigan Street  
Indianapolis, IN 46202

Dr. George R. Inger  
Virginia Polytechnic Institute  
and State University  
Department of Aerospace and  
Ocean Engineering  
Blacksburg, VA 24061

Dr. David S. Ives  
Pratt & Whitney Aircraft  
400 Main Street  
East Hartford, CT 06108

Dr. Antony Jameson  
Courant Institute  
New York University  
New York, NY 10012

Dr. T. Katsanis  
NASA Lewis Research Center  
Cleveland, OH 44135

Dr. J. L. Kerrebrock  
Gas Turbine Laboratory  
Massachusetts Institute of Technology  
Cambridge, MA 02139

Dr. John M. Klineberg  
NASA Headquarters  
600 Independence Avenue  
Washington, DC 20546

Dr. James Krupp  
Middlebury College  
Middlebury, VT 05753

Dr. Metsuru Kurosaka  
General Electric Company  
R&D Center  
Post Office Box 43  
Schenectady, NY 12301

Prof. B. Lakshminarayana  
Pennsylvania State University  
State College, PA 16802

Prof. Frank E. Marble  
California Institute of Technology  
Division of Engineering &  
Applied Sciences  
Pasadena, CA 91109

Dr. William J. McCroskey  
U. S. Army Air Mobility R&D Laboratory  
Moffett Field, CA 94035

Mr. William D. McNally  
NASA Lewis Research Center  
Cleveland, OH 44135

Prof. James E. McCune  
Massachusetts Institute of Technology  
Department of Aeronautics &  
Astronautics  
Gas Turbine Laboratory  
Cambridge, MA 02139

Dr. Robert Melnik  
Grumman Aerospace Corporation  
Bethpage, Long Island, NY 11714

Dr. Gino Moretti  
Polytechnic Institute of New York  
Farmingdale, NY 11735

Dr. Earll M. Murman  
Flow Research, Inc.  
1819 S. Central Avenue  
Kent, WA 98031

Dr. S. N. B. Murthy  
Project Squid Headquarters  
Purdue University  
West Lafayette, IN 47907

Dr. R. A. Novak  
Northern Research and Engineering Corp.  
219 Vassar Street  
Cambridge, MA 02139

Dr. Gordon C. Oates  
University of Washington  
Seattle, WA 98105

Prof. T. H. Okiishi  
Iowa State University of Science  
and Technology  
Department of Mechanical Engineering  
Ames, IA 50010

Prof. R. E. Peacock  
The School of Mechanical Engineering  
Cranfield Institute of Technology  
Cranfield, Bedford  
England

Dr. M. F. Platzer  
U. S. Naval Postgraduate School  
Monterey, CA 93940

Prof. W. D. Rannie  
Karman Laboratory  
California Institute of Technology  
Pasadena, CA 91109

Prof. B. M. Rao  
Texas A&M University  
Department of Aerospace Engineering  
College Station, TX 77843

Prof. N. Rott  
ETH  
Zurich, Switzerland

Dr. A. R. Seebass  
University of Arizona  
Tucson, AZ 85721

Dr. Peter Sokol  
NASA Lewis Research Center  
Cleveland, OH 44135

Dr. J. C. South  
NASA Langley Research Center  
Hampton, VA 23665

Dr. Stephen S. Stahara  
Nielsen Engineering & Research, Inc.  
510 Clyde Avenue  
Mountain View, CA 94040

Mr. H. Starcken  
Institut fur Luftstrahlantriebe  
DFVLR  
Porz-Wahn  
West Germany

Mr. Marvin A. Stibich, AFAPL/TBC  
Air Force Aero Propulsion Laboratory  
Wright-Patterson Air Force Base  
OH 45433

Prof. Demetri P. Telionis  
Virginia Polytechnic Institute &  
State University  
Department of Engineering Sciences  
& Mechanics  
Blacksburg, VA 24061

Dr. W. E. Thompson  
Turbo Research, Inc.  
212 Welsh Pool Road  
Lionville, PA 19353

Dr. Joseph M. Verdon  
United Technologies Research Center  
East Hartford, CT 06108

Mr. Leonard Walitt  
Numerical Continuum Mechanics, Inc.  
Suite 200  
6269 Variel Avenue  
Woodland Hills, CA 91364

Dr. A. Wennerstrom  
Air Force Aero Propulsion Laboratory  
Wright-Patterson Air Force Base  
OH 45433

Dr. H. Yoshihara  
Convair Division  
General Dynamics Corporation  
P.O. Box 80874  
San Diego, CA 92138

Dr. N. J. Yu  
University of Arizona  
Tucson, AZ 85721

UNCLASSIFIED

SECURITY CLASSIFICATION OF THIS PAGE (When Data Entered)

| REPORT DOCUMENTATION PAGE  |  | READ INSTRUCTIONS<br>BEFORE COMPLETING FORM |
|--|--|---|
| 1. REPORT NUMBER<br>AFOSR - TR - 76 - 1082   | 2. GOVT ACCESSION NO.  | 3. RECIPIENT'S CATALOG NUMBER               |
| 4. TITLE (and Subtitle)<br>NONLINEAR SMALL-DISTURBANCE EQUATIONS FOR THREE-DIMENSIONAL TRANSONIC FLOW THROUGH A COMPRESSOR BLADE ROW   | 5. TYPE OF REPORT & PERIOD COVERED<br>INTERIM  |   |
|  | 6. PERFORMING ORG. REPORT NUMBER<br>AB-5487-A-1  |   |
| 7. AUTHOR(s)<br>WILLIAM J RAE  | 8. CONTRACT OR GRANT NUMBER(s)<br>F44620-74-C-0059   |   |
| 9. PERFORMING ORGANIZATION NAME AND ADDRESS<br>CALSPAN CORPORATION<br>P O BOX 235<br>BUFFALO, NEW YORK 14221   | 10. PROGRAM ELEMENT, PROJECT, TASK AREA & WORK UNIT NUMBERS<br>681307<br>9781-01<br>61102F |   |
| 11. CONTROLLING OFFICE NAME AND ADDRESS<br>AIR FORCE OFFICE OF SCIENTIFIC RESEARCH/NA<br>BUILDING 410<br>BOLLING AIR FORCE BASE, D C 20332   | 12. REPORT DATE<br>Aug 76  |   |
|  | 13. NUMBER OF PAGES<br>39  |   |
| 14. MONITORING AGENCY NAME & ADDRESS (if different from Controlling Office)  | 15. SECURITY CLASS. (of this report)<br>UNCLASSIFIED                                       |   |
|  | 15a. DECLASSIFICATION/DOWNGRADING SCHEDULE   |   |
| 16. DISTRIBUTION STATEMENT (of this Report)<br><br>Approved for public release; distribution unlimited.  |  |   |
| 17. DISTRIBUTION STATEMENT (of the abstract entered in Block 20, if different from Report)   |  |   |
| 18. SUPPLEMENTARY NOTES  |  |   |
| 19. KEY WORDS (Continue on reverse side if necessary and identify by block number)<br>TURBOMACHINERY<br>COMPRESSORS<br>TRANSONIC FLOW<br>EQUATIONS   |  |   |
| 20. ABSTRACT (Continue on reverse side if necessary and identify by block number)<br>A derivation is given of the nonlinear, small-disturbance equations governing three-dimensional transonic flow through a fan or compressor rotor. These equations represent the counterpart, for turbomachinery flows, of the small-disturbance equations appropriate to an isolated airfoil. Thus, they facilitate the application to turbomachinery flows of the many numerical solution methods developed in recent years for isolated-airfoil problems. Boundary conditions for design and off-design conditions are formulated, at a level of approximation consistent with the small-disturbance field equations. An order-of-magnitude |  |   |

UNCLASSIFIED

SECURITY CLASSIFICATION OF THIS PAGE (When Data Entered)

**UNCLASSIFIED**

SECURITY CLASSIFICATION OF THIS PAGE(When Data Entered)

analysis is presented, which reveals the transonic similarity parameters for flow in blade rows of low and high solidity. The validity of a rectilinear transonic shear flow as a representation of the flow through a fan or rotor is also discussed.

**UNCLASSIFIED**

SECURITY CLASSIFICATION OF THIS PAGE(When Data Entered)